

## Rhombohedral to simple-cubic phase transition in arsenic under pressure

H. J. Beister, K. Strössner, and K. Syassen

*Max-Planck-Institut für Festkörperforschung, Heisenbergstrasse 1, Postfach 80 06 65,  
D-7000 Stuttgart 80, Federal Republic of Germany*

(Received 2 October 1989)

We have measured powder x-ray diffraction data and Raman spectra of arsenic at pressures up to 33 GPa. X-ray data show a rhombohedral (*A7*) to simple-cubic transition at  $25 \pm 1$  GPa (relative volume  $V/V_0 = 0.772$ ). An upper limit for the volume change  $\Delta V/V_0$  at the transition is given by the experimental uncertainty of 0.5%. We propose an empirical relation between the structural  $u$  parameter and rhombohedral angle  $\alpha$  of the *A7* structure, which is used to estimate the overall variation of first- and second-neighbor bond distances under pressure. The two Raman-active fundamentals of the rhombohedral phase shift to lower frequency for pressures up to 24 GPa, but remain at finite values. Near this pressure, the Raman intensity decreases drastically and the two modes are no longer observed at higher pressures. The Raman data are consistent with a phase transition to a monatomic phase near 25 GPa. Results are discussed in light of several recent first-principles calculations of the phase stability and mode softening of arsenic under pressure.

### I. INTRODUCTION

The semimetallic elements As, Sb, and Bi crystallize in the rhombohedral *A7* (" $\alpha$ -arsenic") crystal structure.<sup>1</sup> This trigonal structure can be derived from a simple-cubic (sc)  $\alpha$ -polonium structure by a rhombohedral distortion along the [111] direction and a simultaneous relative displacement of (111) planes towards each other in pairs along [111] (see Fig. 1), resulting in a distorted octahedral (3+3) coordination. In terms of symmetry the transition from sc to *A7* involves two steps.<sup>2</sup> The first one leads from space group  $Pm\bar{3}m$  to the translationally equivalent subgroup of index 4 (space group  $R\bar{3}m$ , simple rhombohedral  $\beta$ -polonium structure,  $Z=1$ ), the second step leads to the isomorphic subgroup of index 2 ( $Z=2$ ). The *A7* structure can be described as consisting of layers of six-membered rings in chair conformation with intralayer (nearest-neighbor) and interlayer (second-neighbor) bond lengths  $d_1$  and  $d_2$ , respectively. In a covalent picture, the nearly orthogonal bond directions suggest that the bonds are predominantly formed from  $p$  orbitals. The sc-to-*A7* distortion removes  $p$ -orbital degeneracy and results in the formation of three saturated nearest-neighbor bonds.<sup>3</sup>

The suppression of the Peierls-like distortion of the As lattice under hydrostatic pressure, which is expected to eventually result in the formation of a simple-cubic lattice, has been the subject of continuous experimental and theoretical interest.<sup>4-9</sup> An *A7*-to-sc phase transition has been observed in two other group-V elements, at 11 GPa in phosphorous<sup>10,11</sup> and at 7 GPa in antimony.<sup>12</sup> A sc phase is not found among the various high-pressure phases of Bi.<sup>13</sup> In the group of IV-VI binary compounds an analogous phase change from the rhombohedral to the NaCl-type structure induced by temperature<sup>14</sup> or pressure<sup>15</sup> is reported, e.g., GeTe and SnTe, and the ferroelectric properties and soft-mode behavior of these polar ma-

terials have been studied in detail.<sup>16</sup> The ratios  $d_2/d_1$  listed in Table I indicate a larger stability of the *A7* structure with respect to sc in As as compared to Sb and Bi. Hence, one expects an *A7*-sc transformation in As to take place at higher pressures than in Sb.

For As it was shown earlier that the *A7* x-ray diffraction pattern changes gradually under pressure in the direction towards a sc one.<sup>4,5</sup> A metastable tetragonal phase of As has been reported,<sup>20</sup> which is obtained by pressure quenching from about 15 GPa. Its structure is possibly similar to that of the Sb-III phase stable between 8.5 and 28 GPa.<sup>21,22</sup> The pressure dependence of the superconducting transition temperature of As measured by Wittig and co-workers<sup>23,24</sup> indicates a phase change at about 20–24 GPa. Several first-principles calculations of the relative stability of the *A7* and sc structure of As have been reported recently.<sup>6-8</sup> These calculations show that the lowering of symmetry from sc to *A7* goes along with a splitting of the  $4p$  valence states and a strong decrease of the electronic density of states near the Fermi

TABLE I. Crystallographic data for the rhombohedral phase (space group  $R\bar{3}m$ ) of As, Sb, and Bi at normal pressure and  $T=293$  K. The axes refer to a trigonal setting of the unit cell.

Parameter	As <sup>a</sup>	Sb <sup>b</sup>	Bi <sup>c</sup>
$a$ (pm)	375.98	430.84	454.6
$c$ (pm)	1054.75	1127.4	1186.2
$u$ parameter	0.227 07	0.233 49	0.233 92
$d_1$ (pm)	251.6	290.8	307.1
$d_2$ (pm)	312.1	335.5	352.9
$d_2/d_1$	1.240	1.154	1.149

<sup>a</sup>Reference 17.

<sup>b</sup>Reference 18.

<sup>c</sup>Reference 19.

level  $E_F$ . The corresponding lowering of the band-structure energy then stabilizes the rhombohedral distortion.<sup>7,8</sup> The calculations of Needs *et al.*<sup>6</sup> performed for relative volumes  $V/V_0 > 0.8$  show the  $A7$  structure to be more stable relative to sc. Chang and Cohen<sup>7</sup> predict that at about  $V/V_0 = 0.72$  ( $P \approx 35$  GPa) the sc phase will become stable against a second-order-like displacive transition towards an  $A7$  structure. According to Mattheiss *et al.*<sup>8</sup> an  $A7$ -to-sc transition is predicted at  $V/V_0 = 0.8$  ( $P \approx 19$  GPa). More recent energy-dispersive x-ray diffraction studies suggest<sup>9</sup> that the  $A7$  structure of As is stable up to 34 GPa ( $V/V_0 = 0.74$ ), where it undergoes a transition to sc involving a large discontinuity in specific volume of about 5%.

In this paper we report an independent angle-dispersive powder x-ray diffraction (XRD) study and a

Raman investigation of As for pressures up to  $\sim 30$  GPa. The motivation for a combined XRD and Raman study is as follows: (i) In general terms, a phase transition from  $A7$  to sc in As may be considered as a prototype example for a pressure-induced suppression of a Peierls-type distortion in a layered elemental solid involving a semimetal-to-metal transition as well as strong electron-phonon coupling and phonon softening (see, e.g., Refs. 6 and 7). (ii) The apparent discrepancy between the stability of the  $A7$  structure up to  $\sim 34$  GPa (Ref. 9) and a possible phase transition near 20–24 GPa as indicated by the superconducting behavior<sup>23,24</sup> needs to be explained. (iii) Arsenic in the  $A7$  structure has two Raman-active zone-center phonon modes.<sup>25</sup> High-pressure Raman spectroscopy not only provides important information on the softening<sup>6,26</sup> of these modes, but also gives independent evidence for the occurrence of a structural phase transition. In particular, a pressure-induced transition to the sc or simple rhombohedral structure is expected to manifest itself in a vanishing of the Raman activity due to zone-center optical modes. (iv) The recent application of various first-principles calculational methods<sup>6–8</sup> to the problem of phase stability, structural properties, and phonons of  $A7$ -As stimulates detailed studies of the high-pressure behavior of As using different experimental methods.

The paper is organized as follows: After giving some experimental details (Sec. II), the XRD results are presented in Sec. III and the pressure dependence of Raman-active phonons is discussed in Sec. IV.

## II. EXPERIMENTAL DETAILS

Samples for high-pressure studies were prepared from a Bridgman-grown single crystal. A gasketed diamond-window high-pressure cell<sup>27</sup> was used for both x-ray diffraction and Raman measurements. Samples were embedded in a 4:1 methanol-ethanol pressure medium, which provides hydrostatic conditions up to  $\sim 10$  GPa and nearly isotropic conditions at higher pressures. Pressures were measured by the standard ruby luminescence method.<sup>28</sup> For XRD investigations the single-crystal material was powdered. The powder pattern was observed down to a  $d$  spacing of 130 pm using an angle-dispersive diffraction geometry (Debye-Scherrer method, filtered Mo  $K\alpha$  radiation) and a position-sensitive proportional counter system. Experimental errors in absolute lattice parameters and unit-cell volumes are estimated to be  $\sim 0.15$  and  $\sim 0.5$ %, respectively. Raman measurements were performed in backscattering geometry with the cleaved basal plane of a single-crystal sample oriented perpendicular to the laser beam. The excitation wavelength was 514.5 or 488 nm. Raman spectra were measured with a multichannel spectrometer system (Mepsicon imaging resistive anode photomultiplier coupled to a Spex triplemate spectrometer). All measurements were made at room temperature.

## III. X-RAY DIFFRACTION RESULTS

In discussing the results of x-ray diffraction studies we refer to both the rhombohedral and the trigonal setting of

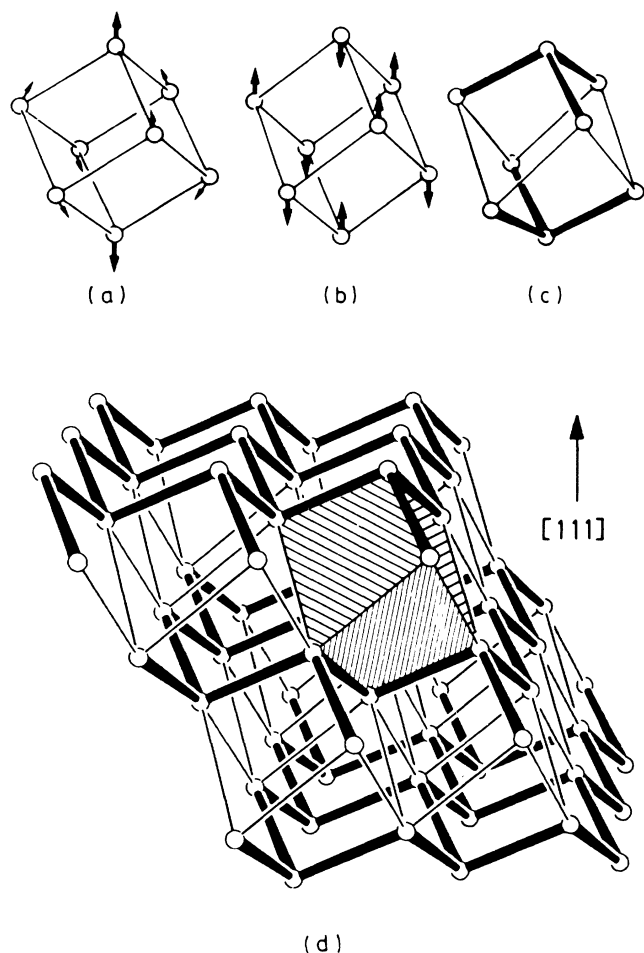


FIG. 1. The rhombohedral  $A7$  structure of As can be derived from the simple-cubic lattice (a) by a rhombohedral distortion along the  $[111]$  direction and (b) a pairing of  $(111)$  lattice planes along the same direction. The resulting structure [(c) and (d)] consists of buckled layers with in-plane bond length  $d_1$  (heavy lines) and interlayer nearest-neighbor bond length  $d_2$ . Shaded planes in (d) indicate the distorted cube. The  $[111]$  direction refers to both the sc lattice and the  $A7$  lattice in the rhombohedral setting.

the space group  $R\bar{3}m$ . In terms of the rhombohedral lattice parameter  $a_{\text{rhom}}$  and angle  $\alpha_{\text{rhom}}$  the trigonal lattice parameters are given by

$$\begin{aligned} a_{\text{trig}} &= 2a_{\text{rhom}} \sin(\alpha_{\text{rhom}}/2), \\ (c/a)_{\text{trig}} &= \{9[4 \sin^2(\alpha_{\text{rhom}}/2)]^{-1} - 3\}^{1/2}. \end{aligned} \quad (1)$$

In the rhombohedral description the atoms occupy the Wyckoff<sup>29</sup>  $2c$  sites  $\pm(u, u, u)$ , in the trigonal setting the  $6c$  sites  $\pm(0, 0, u)$ . The simple-cubic structure is given by  $u=0.25$  and by  $\alpha=60^\circ$  or  $c/a = \sqrt{2} \times \sqrt{3}$ . For more details about the various descriptions of the  $A7$  structure see Refs. 6 and 8.

The lattice parameters of As were determined from the strongest observed Bragg reflections by least-squares methods. Up to 3 GPa the (113), (015), (110), (104), and (012) reflections were taken into account. At higher pressures, lattice parameters were calculated from the (110), (104), and (012) reflections only, because the other reflections became very weak. Under these conditions the very gradual change of the diffraction pattern from  $A7$  towards sc requires a careful analysis of the (110) and (104) reflections in order to determine the pressure at which the  $A7$ -sc phase transition occurs. Figure 2 shows the  $2\theta$  distance  $\Delta_1$  of the (110) and (104) reflections and the distance of both reflections with the added  $\frac{1}{2}$  full width at half maximum (FWHM) of each peak ( $\Delta_2$ ) as a function of pressure. With increasing pressure, the  $2\theta$  splitting  $\Delta_1$  becomes smaller. At 25 GPa the peak distance decreases rapidly by  $0.35^\circ$  as indicated by the corresponding change in the total width  $\Delta_2$  of the two overlapping reflections. Above 25 GPa we observe a peak profile

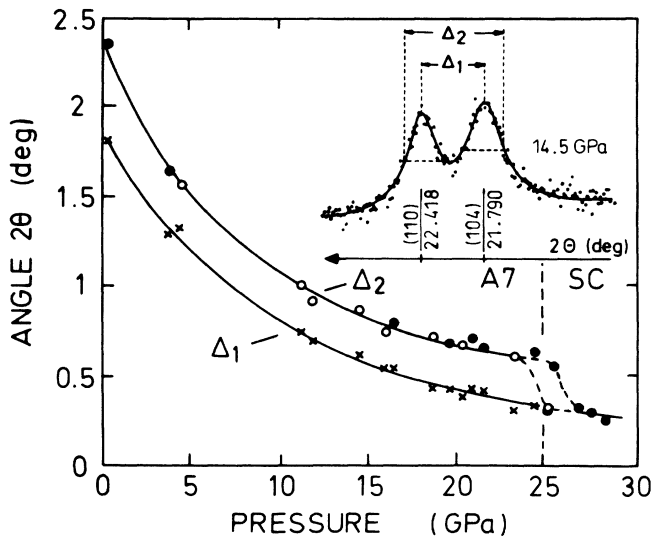


FIG. 2. Pressure dependence of x-ray diffraction peaks of As. The lower curve (crosses) gives the  $2\theta$  splitting  $\Delta_1$  between (110) and (104) reflections in the  $A7$  structure ( $P < 25$  GPa). The upper curve (circles) represents the angle difference  $\Delta_2$  between points taken at half-height at the low and high angle side of the (104) and (110) reflections, respectively (see inset). Open and solid circles represent data from two different runs.

typical for a single diffraction line and the FWHM remains essentially constant as the pressure increases further. Thus, we conclude that the phase transition from the rhombohedral  $A7$  structure to the sc phase occurs near 25 GPa, where the (110) and (104) reflections of the  $A7$  structure merge into the (110) reflection of the sc lattice. At pressures above 25 GPa we observe the three reflections (100), (110), and (111) of the simple-cubic lattice. For two different sample loadings the transitions pressure differed by less than 1.5 GPa. The phase transition is reversible. For decreasing pressure the splitting of the cubic (110) reflection is clearly observed again at 23 GPa. Thus, any hysteresis in the phase change is less than 2 GPa. We can rule out the possibility of an intermediate simple rhombohedral phase.

The relative change of the trigonal lattice parameters  $a$  and  $c$  as a function of pressure is shown in Fig. 3. For the cubic lattice we give the  $a$  and  $c$  parameters for the (pseudo-) trigonal setting with  $a_{\text{trig}} = a_{\text{cub}} \sqrt{2}$  and  $c_{\text{trig}} = 2a_{\text{cub}} \sqrt{3}$ . The solid lines for the  $A7$  phase refer to the result of fitting the one-dimensional analog of a Murnaghan-type relation<sup>30</sup> to the experimental data. Parameters are given in Table II. There is substantial disagreement between our parameters  $\beta_0$  and inverse linear compressibilities derived from low-pressure x-ray data<sup>4</sup> as well as elastic constants<sup>31</sup> at ambient pressure

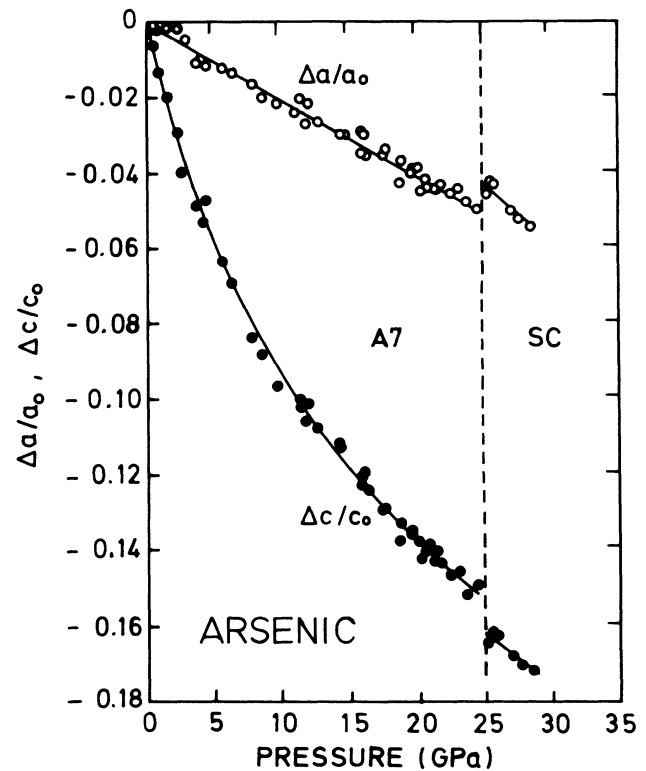


FIG. 3. Relative change of the  $a$  and  $c$  axes of As as a function of pressure. Axes refer to the trigonal setting. Solid lines represent the results of least-squares fits of a Murnaghan-type relation (Ref. 30) to the experimental data (see Table II for parameters).

TABLE II. Summary of experimental and calculated high-pressure properties of arsenic. The quantities  $B_0$  and  $B'_0$  are bulk modulus and its pressure derivative at zero pressure, respectively, and  $\beta_0$  and  $\beta'$  are the inverse linear compressibility and its pressure derivative (see Ref. 30) for compression parallel and perpendicular to the trigonal axis. The quantities  $P_T$  and  $V_T/V_0$  are pressure and relative volume, respectively, at the  $A7$ -to-sc phase transition.

Property	Experiment		Calculation
	This work	Literature	
$B_0$ (GPa)	58(4)	59 <sup>a</sup> , 38 <sup>b</sup> , 55.6 <sup>c</sup>	43 <sup>d</sup> , 77 <sup>e</sup>
$B'$	3.3(4)	4.4 <sup>c</sup>	
$\beta_{0\parallel}$ (GPa)	470(10)	-210 <sup>a</sup> , 910 <sup>b</sup>	
$\beta'_{\parallel}$	1 (fixed)		
$\beta_{0\perp}$ (GPa)	63(2)	38 <sup>a</sup> , 42 <sup>b</sup>	
$\beta'_{\perp}$	9.4(4)		
$P_T$ (GPa)	25(1)	~34 <sup>c</sup>	19 <sup>e</sup> , 35 <sup>f</sup>
$V_T/V_0$	0.772		0.80 <sup>e</sup> , 0.72 <sup>f</sup>

<sup>a</sup>Reference 31 (elastic constants).

<sup>b</sup>Reference 4 (single-crystal XRD,  $P=0.31$  GPa).

<sup>c</sup>Reference 9 (powder XRD,  $P \leq 40$  GPa).

<sup>d</sup>Reference 6.

<sup>e</sup>Reference 8.

<sup>f</sup>Reference 7.

(see Table II). High-resolution lattice-parameter measurements would be helpful in clarifying the situation, in particular, with respect to a possible anomalous compression behavior of As at low pressures.

The strongly different axial compressibilities in the  $A7$  phase (Fig. 3) obviously reflect the difference between weak interlayer and stronger intralayer bonding. At the  $A7$ -to-sc transition we find an increase of the  $a$  axis by about 0.5% and a decrease of the  $c$  axis which is about twice as large. The lattice constants at the phase transition are  $a_{\text{trig}} = 358.9(5)$  pm and  $c_{\text{trig}} = 893.7(13)$  pm for the  $A7$  phase and  $a_{\text{cub}} = 255.0(4)$  pm. The latter value is slightly larger compared to the shorter bond length in As at normal pressure (see Table I).

Within experimental uncertainty of 0.5% in volume, we observe no discontinuity in the change of the relative volume  $V/V_0$ , as shown in Fig. 4. The solid line refers to the result of fitting a Murnaghan relation<sup>30</sup> to the experimental data (see Table II for parameters). For the bulk modulus  $B_0$  we find good agreement between the present result and data of Ref. 9. At the phase transition the relative volume of the  $A7$  phase [ $V/V_0 = 0.772(7)$ ] is slightly below the transition volume at  $T=0$  K ( $V/V_0 = 0.8$ ) calculated by Mattheiss *et al.*<sup>8</sup>

Figure 5 shows the rhombohedral angle  $\alpha$  as a function of relative volume  $V/V_0$ . The angle  $\alpha$  increases steadily from  $54.13^\circ$  at ambient pressure to  $59^\circ$  just before the phase transition, where it adopts the cubic value of  $\alpha = 60^\circ$ . We note the surprisingly good agreement between present results and earlier work of McWhan<sup>5</sup> (see Fig. 5) who just reports the variation of  $\alpha$  for volumes down to  $V/V_0 \approx 0.8$  without giving further details of his work like pressure-volume data, etc.

A determination of the free  $u$  parameter of the arsenic

structure from powder data is difficult, because absorption and some preferential orientation effects lead to uncertain intensities of x-ray diffraction peaks. As a consequence we do not attempt to directly determine the variation of the bond lengths of As in the  $A7$  structure from the present experimental data.

Intuitively, one may expect that the variation of the  $u$  parameter is coupled to the change in the rhombohedral angle  $\alpha$ , because both quantities are a measure of the distortion from simple cubic induced by the same chemical bonding scheme. We propose an empirical relation between the  $u$  parameter and  $\alpha$  of the  $A7$  structure given by the solid line in Fig. 6(a). The relation is obtained from the zero-pressure structural data<sup>17-19</sup> for the group-V elements (300 and 4 K) and the assumption that  $u = 0.25$  for  $\alpha = 60^\circ$ . This  $u(\alpha)$  dependence appears reasonable because (i) the experimental data for Sb under pressure<sup>32,33</sup> follow the empirical relation, at least for  $\alpha < 59^\circ$ , and (ii) the calculated values of Needs *et al.*<sup>6</sup> for As suggest a very similar behavior, except for a small offset to lower  $u$  values [see Fig. 6(a)]. Based on the empirical  $u(\alpha)$  rela-

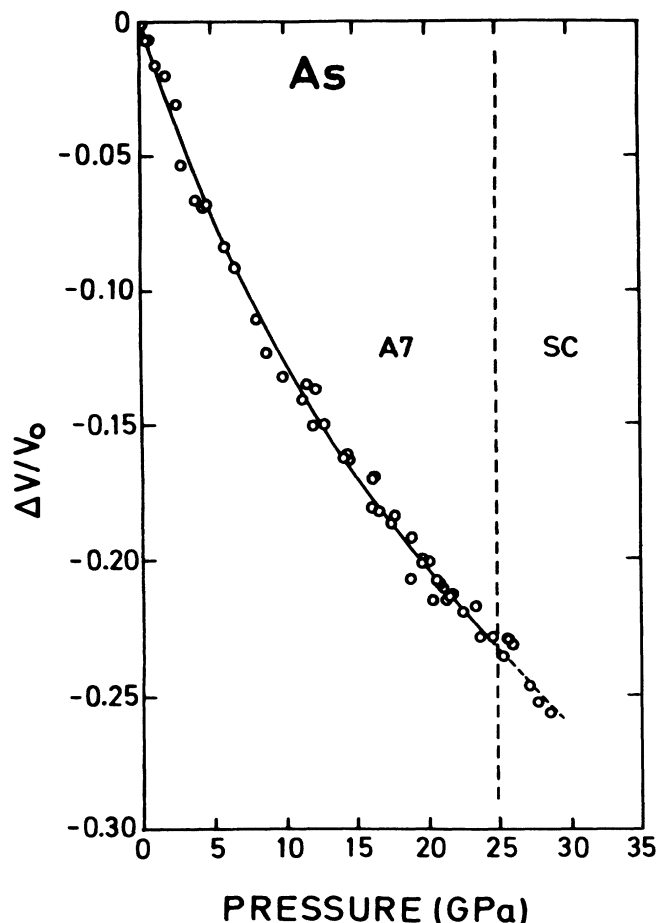


FIG. 4. The pressure-volume relation of arsenic at 300 K. The solid line represents the result of a least-squares fit of a Murnaghan equation (Ref. 30) to the experimental data (see Table II for parameters).

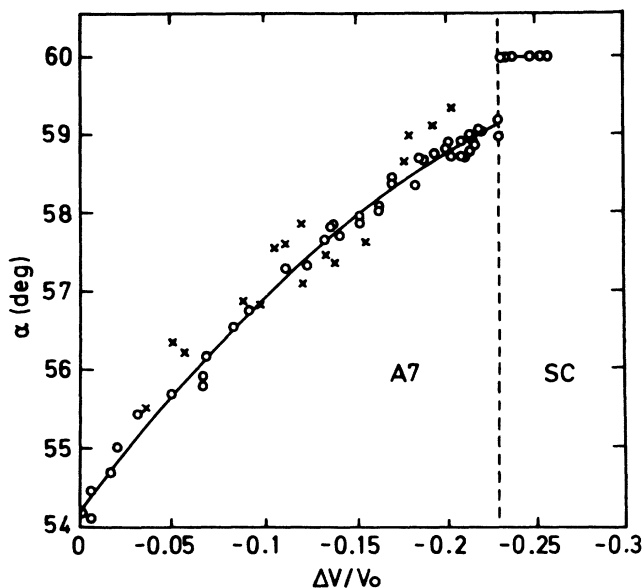


FIG. 5. The rhombohedral angle  $\alpha$  of As as a function of volume. Solid line is a guide to the eye for present data points (open circles). Crosses represent earlier data by McWhan (Ref. 5).

tion we estimate the relative changes of the distances  $d_1$  and  $d_2$  between first- and second-nearest-neighbor atoms as a function of pressure, as shown in Fig. 6(b). The distance  $d_2$  decreases monotonically, by about 15% up to 25 GPa. The distance  $d_1$  also decreases throughout the stability range of the  $A7$  structure, the maximum change, however, being only  $-1.5\%$  at 25 GPa. At the  $A7$ -to- $sc$  transition  $d_2$  decreases by  $\sim 3\%$ , whereas the shortest bond length  $d_1$  increases by  $\sim 2.5\%$ . This behavior is reasonable in view of the general tendency shown by covalent solids where a pressure-induced breakdown of directional bonding and increase in coordination number results in an increase of the nearest-neighbor bond distance.

Morosin and Schirber<sup>4</sup> have obtained the change of the  $u$  parameter from single-crystal investigations of As for pressures up to 0.31 GPa. They find an increase of  $u$  in qualitative agreement with the empirical  $u(\alpha)$  relation proposed above. A quantitative comparison of distances  $d_1$  and  $d_2$  with those derived from their data is not meaningful because their axial compressibilities differ significantly from the corresponding results obtained in this study (see Table II).

We emphasize that the pressure dependences of bond distances shown in Fig. 6(b) is only an *estimate* of the overall behavior in the stability range of the  $A7$  structure. Single-crystal diffraction studies of As performed for a larger pressure range compared to that covered in Ref. 4 may well reveal more subtle effects in the pressure dependence of the bond lengths.

In closing this section, we note that under the nearly hydrostatic conditions of our experiment we did not observe the tetragonal phase of As.<sup>20</sup> However, no attempts were made to investigate the existence of this

phase under strongly nonhydrostatic conditions or under rapid decompression. The results for the pressure dependence of the superconducting transition temperature  $T_c$  obtained in an earlier investigation<sup>34</sup> differ from those of Wittig.<sup>23,24</sup> This possibly indicates that under certain conditions a different phase may be present in As at pressures above 12 GPa. Furthermore, it remains to be investigated, whether As at very high pressures undergoes the predicted transition<sup>35</sup> from  $sc$  to  $bcc$ , which is also observed for Sb (Ref. 22) and Bi (Ref. 9) near 28 and 7.7 GPa, respectively.

#### IV. RAMAN SPECTRA UNDER PRESSURE

The rhombohedral lattice of arsenic with two atoms per unit cell has three Raman-active zone-center modes,<sup>25,26</sup> an  $A_{1g}$  mode at  $\sim 253$ – $257$   $\text{cm}^{-1}$  and a two-

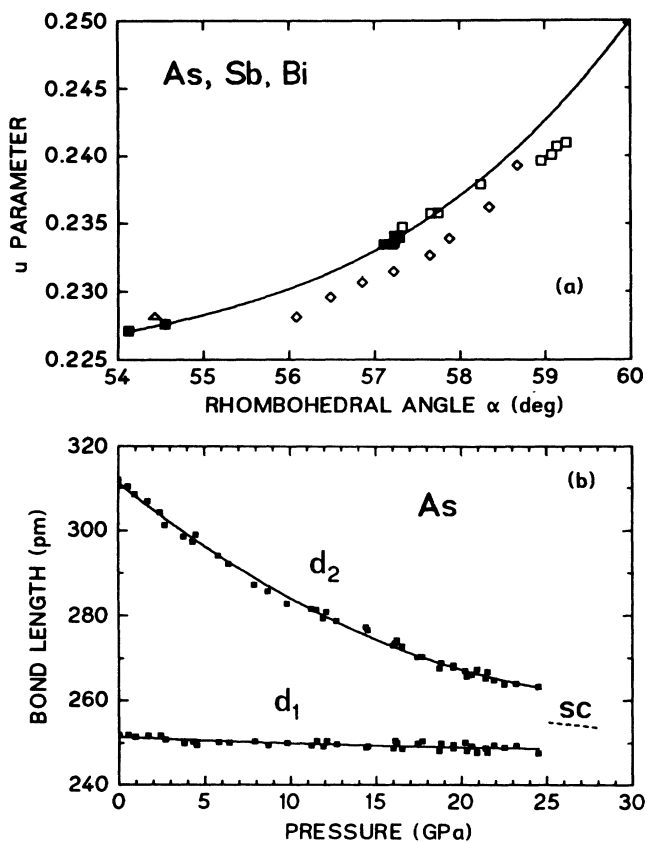


FIG. 6. (a) Internal parameter  $u$  as a function of the rhombohedral angle  $\alpha$  for group-V elemental solids. Solid symbols refer to zero-pressure data at 300 and 4 K and the solid line is a smooth curve through these points including the simple-cubic point. Open squares correspond to high-pressure data for Sb (Refs. 31 and 32). Open diamonds represent calculated results for As (Ref. 6) and the triangle refers to the result of Ref. 4. (b) First- and second-nearest-neighbor distance in rhombohedral As as a function of pressure, as calculated from the experimental lattice parameters under pressure using the empirical  $u(\alpha)$  relation shown by the solid line in (a). The dashed line represents the simple-cubic lattice constant.

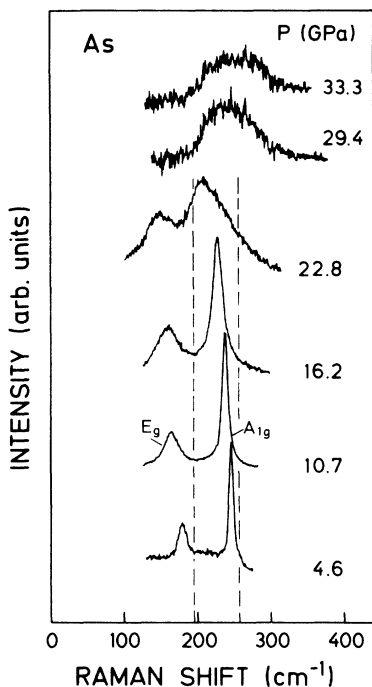


FIG. 7. Raman spectra of arsenic at different pressures ( $T=300$  K). Vertical dashed lines indicate Raman shifts of the  $E_g$  and  $A_{1g}$  modes at zero pressure.

fold degenerate  $E_g$  mode at  $\sim 193$ – $197$   $\text{cm}^{-1}$ . For phonons propagating along the trigonal axis (i.e., perpendicular to the layers) of the rhombohedral lattice, the  $A_{1g}$  mode belongs to a pure longitudinal motion of the atom planes and thus is related to the Peierls-like atomic displacements as indicated by arrows in Fig. 1(b). In the sc lattice, this mode corresponds to LA phonons with wave vector at the corner ( $R$  point) of the Brillouin zone. The two  $E_g$  modes of the  $A7$  lattice correspond to transverse motions. Raman scattering experiments at moderate pressures ( $P \leq 0.7$  GPa) have shown that both modes soften with increasing pressure,<sup>26</sup> a behavior which is also predicted for the  $A_{1g}$  mode on the basis of total energy calculations using the frozen phonon method.<sup>6</sup>

Raman spectra of As at different pressures are shown in Fig. 7. We find the frequencies of the two optical modes at normal pressure  $\omega_0(A_{1g})=256(1)$   $\text{cm}^{-1}$  and  $\omega_0(E_g)=196(1)$   $\text{cm}^{-1}$  in agreement with Zitter<sup>25</sup> and

$$b = -2.3(1) \text{ cm}^{-1}/\text{GPa}, \quad c = 0.05(1) \text{ cm}^{-1}/\text{GPa}^2 \text{ for the } A_{1g} \text{ mode,}$$

$$b = -4.0(2) \text{ cm}^{-1}/\text{GPa}, \quad c = 0.11(2) \text{ cm}^{-1}/\text{GPa}^2 \text{ for the } E_g \text{ mode.}$$

The mode softening becomes more pronounced, especially for the transverse  $E_g$  mode, in the pressure range between 20 and 24 GPa, where the line width also increases significantly (see spectra in Fig. 7). Under the given experimental conditions (quasihydrostatic pressure), the two mode frequencies remain at finite value at the phase

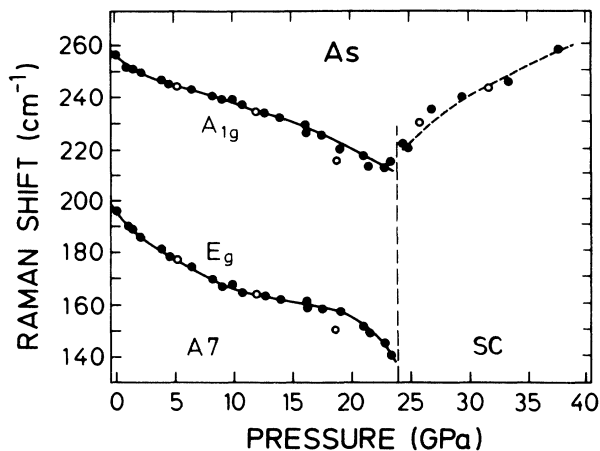


FIG. 8. Raman line frequencies of arsenic as a function of pressure. Data below 25 GPa refer to the two Raman-active modes of rhombohedral As. In the simple-cubic phase, stable above 25 GPa, only a very weak and broad band is observed (see Fig. 7) and the corresponding data refer to the Raman shift of its maximum. Solid and dashed lines through the data points are a guide to the eye.

Richter *et al.*<sup>26</sup> For increasing pressure, both optical modes decrease in frequency, the total relative shift being about  $-17$  and  $-30\%$  for the  $A_{1g}$  and  $E_g$  modes, respectively, at 24 GPa. For pressures above  $\sim 24$  GPa, the two Raman modes of  $A7$ -As vanish, consistent with a change of crystal symmetry. At higher pressures we observe only a broad feature, which is very weak as evidenced by the decrease of the signal-to-noise ratio of the spectra in Fig. 7. This band moves to higher frequency with increasing pressure. Within the mutual uncertainty of the two experiments, the phase-transition pressure determined from Raman measurements ( $\sim 24$  GPa) agrees with the x-ray diffraction result reported above.

The pressure dependence of the two mode frequencies in the  $A7$  phase, as well as the frequency of the broad Raman band observed in the sc phase, are shown in Fig. 8. In agreement with the results obtained by Richter *et al.*<sup>26</sup> in the pressure range up to 0.7 GPa the initial decrease in mode frequency is stronger for the  $E_g$  mode compared to the  $A_{1g}$  mode. Up to 10 GPa the pressure dependence is sublinear and can be described by  $\Delta\omega(P)=b \cdot P + c \cdot P^2$  with first- and second-order coefficients given by

transition. The pressure shift of the Raman bands is reversible upon decreasing the pressure.

The broad Raman band in the sc phase is likely to arise from disorder-induced scattering, thus reflecting a maximum in the phonon density of states. This interpretation is supported by the fact that as a function of pressure

the frequency of the  $A_{1g}$  mode joins smoothly into the frequency of the broad band in simple cubic, as would be expected due to the unfolding of the Brillouin zone at the  $A7$ -to-sc transition.

Figure 9 shows the dependence of the  $A7$  mode frequencies as a function of relative volume  $V/V_0$ . The slope in the linear part of the frequency versus volume data ( $0.88 \leq V/V_0 \leq 1$ ) corresponds to average mode Grüneisen parameters  $\bar{\gamma} = -(\Delta\omega/\omega_0)/(\Delta V/V_0)$  of

$$\bar{\gamma} = -0.45(5) \text{ for the } A_{1g} \text{ mode}$$

and

$$\bar{\gamma} = -1.15(5) \text{ for the } E_g \text{ mode.}$$

The overall dependence of the  $A_{1g}$  mode frequency on volume is similar to the behavior calculated by Needs *et al.*<sup>6</sup> (see dashed line in Fig. 9), but the mode softening is less pronounced in the experimental results. In the calculation of Chang and Cohen<sup>7</sup> the stability of the sc phase was investigated in terms of total energy changes with respect to the longitudinal phonon displacement (see Fig. 1) corresponding to the sc-to- $A7$  distortion. The force constant for this phonon displacement was found to

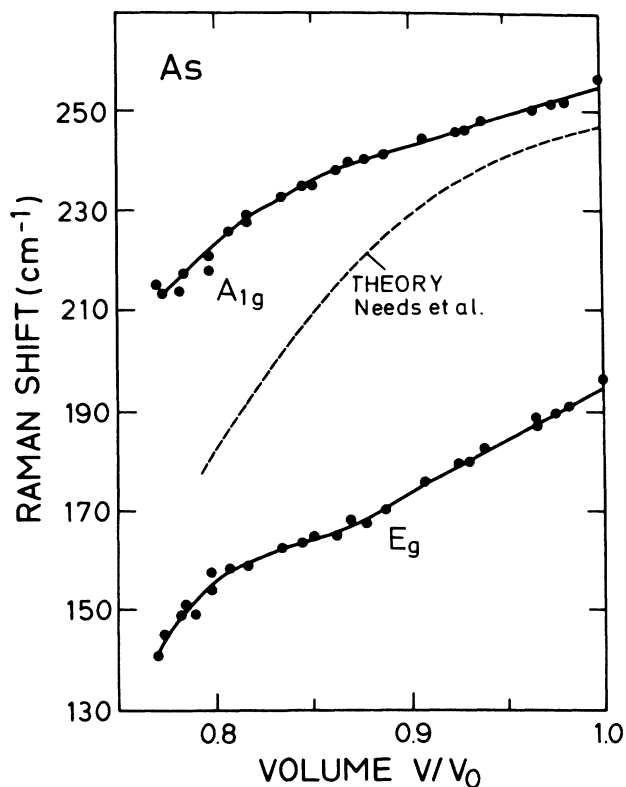


FIG. 9. Raman line frequencies of As in the  $A7$  phase as a function of relative volume. Solid lines are a guide to the eye. The slope in the straight line sections for  $0.88 < V/V_0 < 1$  corresponds to mode Grüneisen parameters  $\gamma(A_{1g}) = -0.45$  and  $\gamma(E_g) = -1.15$ . The dashed line for the  $A_{1g}$  mode is taken from the calculation of Needs *et al.* (Ref. 6).

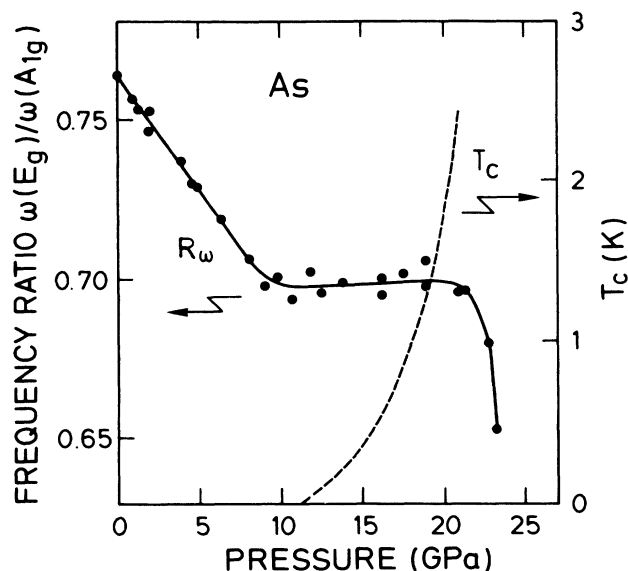


FIG. 10. The ratio  $R_\omega$  of the  $E_g$  and  $A_{1g}$  phonon frequencies of As as a function of pressure. The solid line is a guide to the eye. The dashed line gives the variation of the superconducting transition temperature according to Wittig (Ref. 23).

become positive (corresponding to the stability of the sc lattice) only at pressures above 35 GPa. Thus, this treatment of the relative stability of  $A7$  and sc in terms of a second-order displacive phase transition overestimates the transition pressure.

Figure 10 shows the ratio of the Raman frequencies  $R_\omega = \omega(E_g)/\omega(A_{1g})$  of the  $A7$  phase as a function of pressure. The frequency ratio  $R_\omega$  decreases from 0.76 at normal pressure to 0.69 at about 10 GPa, and then remains nearly constant up to 22 GPa, which is close to the phase-transition pressure. Differences in electron-phonon coupling for the longitudinal and transverse modes may be responsible for the peculiar pressure dependence of the frequency ratio  $R_\omega$ . The pressure dependence of the lattice parameters (see Fig. 3) does not show, within experimental accuracy, any evidence for anomalous behavior near 10 GPa. This, however, does not rule out the possibility that subtle effects in the first- and second-neighbor bond distances are related to the change in slope of the pressure dependence of the frequency ratio  $R_\omega$  near 10 GPa. The linewidth of the Raman lines increases continuously with pressure, in particular, close to the phase transition; this may be another indication for an increasing electron-phonon coupling under pressure.

In this context we point out that As is observed to become superconducting near 11 GPa and the transition temperature raises steadily up to 2.5 K at about 20 GPa (see data of Ref. 23 shown in Fig. 10). Thus, there is a near coincidence between the onset of superconductivity and the change of slope of the  $R_\omega(P)$  curve in Fig. 10. At about 20–24 GPa  $T_c$  becomes independent of pressure, which was taken as an indication for a structural phase transition.<sup>23,24</sup> At around 20 GPa the pressure in the  $T_c$

measurements is probably underestimated by 10–15 % relative to the ruby scale used in the present experiment.<sup>36</sup> Thus, we find excellent agreement between phase-transition pressures observed in our x-ray diffraction and Raman scattering experiments and the indirect evidence for a phase transition from the  $T_c$  measurements of Refs. 23 and 24.

## V. CONCLUSIONS

We have performed x-ray diffraction and Raman studies of As under pressure ( $T=300$  K). X-ray diffraction data show a phase transition from the  $A7$  to the sc phase at  $P_T=25\pm 1$  GPa ( $V/V_0=0.772$ ). This value is significantly lower than the previous experimental results of  $32$  GPa  $< P_T < 36$  GPa,<sup>9</sup> but in good agreement with a phase transition indicated by the pressure dependence of the superconducting transition temperature.<sup>23,24</sup> The upper limit for the volume change at the phase change is less than 0.5%, much lower than the value of 5% reported in Ref. 9. We propose an empirical relation between the  $u$  parameter and rhombohedral angle  $\alpha$  of the  $A7$  structure, which is used to roughly estimate the overall change of first- and second-neighbor distances in the  $A7$  phase as a function of pressure. The frequencies of the

Raman-active  $A_{1g}$  and  $E_g$  zone-center phonons of the  $A7$  lattice decrease by about 17 and 30 %, respectively, for pressures between 0 and 24 GPa. The frequency ratio of the Raman modes when plotted as a function of pressure, shows a pronounced change in slope near 10 GPa, which is close to the onset of superconductivity in As. The softening of the  $A_{1g}$  mode under pressure is qualitatively similar, but less pronounced, compared to the behavior predicted in first-principles calculations.<sup>6</sup> Except for a very weak and broad band which we attribute to disorder-induced scattering, Raman modes are no longer observed at pressures above 24 GPa. Thus, the Raman data are consistent with a transition to a simple-cubic phase near this pressure. X-ray and Raman data suggest that the  $A7$ -to-sc transition is of first order or very close to first order. Under pressure, As exhibits pronounced changes in the optical response, both in the stability range of the  $A7$  phase and at the  $A7$ -sc transition.<sup>37</sup> These results will be reported in a forthcoming paper.

## ACKNOWLEDGMENTS

We thank E. Schönherr for growing single crystals of arsenic and W. Böhringer, W. Dieterich, and S. Heymann for help in the experiments.

- <sup>1</sup>J. Donohue, *The Structure of the Elements* (Wiley, New York, 1974).
- <sup>2</sup>H. Bärninghausen, *Match* **9**, 139 (1980).
- <sup>3</sup>P. B. Littlewood, *J. Phys. C* **13**, 4855 (1980); **13**, 4875 (1980).
- <sup>4</sup>B. Morosin and J. E. Schirber, *Solid State Commun.* **10**, 249 (1972).
- <sup>5</sup>D. B. McWhan, *Science* **176**, 751 (1972).
- <sup>6</sup>R. J. Needs, R. M. Martin, and O. H. Nielsen, *Phys. Rev. B* **33**, 3778 (1986); **35**, 9851 (1987).
- <sup>7</sup>K. J. Chang and M. L. Cohen, *Phys. Rev. B* **33**, 7371 (1986).
- <sup>8</sup>L. F. Mattheiss, D. R. Hamann, and W. Weber, *Phys. Rev. B* **34**, 2190 (1986).
- <sup>9</sup>T. Kikegawa and H. Iwasaki, *J. Phys. Soc. Jpn.* **56**, 3417 (1987).
- <sup>10</sup>J. Jamieson, *Science* **139**, 1291 (1963).
- <sup>11</sup>T. Kikegawa and H. Iwasaki, *Acta Crystallogr. B* **39**, 158 (1983).
- <sup>12</sup>T. N. Kolobyanina, S. S. Kabalkina, L. F. Vereshchagin, and L. V. Fedina, *Zh. Eksp. Teor. Fiz.* **55**, 164 (1968) [*Sov. Phys.—JETP* **28**, 88 (1969)].
- <sup>13</sup>K. Aoki, S. Fujiwara, and M. Kusakabe, *J. Phys. Soc. Jpn.* **51**, 3826 (1982), and references therein.
- <sup>14</sup>T. Chattopadhyay, J. X. Boucherle, and H. G. v. Schnering, *J. Phys. C* **20**, 1431 (1987), and references therein.
- <sup>15</sup>S. S. Kabalkina, L. F. Vereshchagin, and N. R. Serebryanaya, *Zh. Eksp. Teor. Fiz.* **51**, 1358 (1966) [*Sov. Phys.—JETP* **24**, 917 (1967)].
- <sup>16</sup>K. M. Rabe and J. D. Joannopoulos, *Phys. Rev. B* **32**, 2302 (1985), and references therein; W. Jantsch, in *Dynamical Properties of IV-VI Compounds*, Vol. 99 of *Springer Tracts in Modern Physics* (Springer, Berlin, 1983), p. 1; A. Bussmann-Holder, H. Bilz, and P. Vogl, *ibid.*, p. 51.
- <sup>17</sup>D. Schiferl and C. S. Barrett, *J. Appl. Cryst.* **2**, 30 (1969).
- <sup>18</sup>C. S. Barrett, P. Cucka, and K. Haefner, *Acta Crystallogr.* **16**, 451 (1963).
- <sup>19</sup>P. Cucka and C. S. Barrett, *Acta Crystallogr.* **15**, 865 (1962).
- <sup>20</sup>M. J. Duggin, *J. Phys. Chem. Solids* **33**, 1267 (1972).
- <sup>21</sup>S. S. Kabalkina, T. N. Kobobyanina, and L. F. Vereshchagin, *Zh. Eksp. Teor. Fiz.* **58**, 486 (1970) [*Sov. Phys.—JETP* **31**, 259 (1970)].
- <sup>22</sup>K. Aoki, S. Fujiwara, and M. Kusakabe, *Solid State Commun.* **45**, 161 (1983).
- <sup>23</sup>J. Wittig, in *High Pressure Science and Technology*, edited by C. Homan, R. K. MacCrone, and E. Whalley (North-Holland, New York, 1984), Pt. I, p. 17.
- <sup>24</sup>H. Kawamura and J. Wittig, *Physica B+C* **135**, 239 (1985).
- <sup>25</sup>R. N. Zitter, in *The Physics of Semimetals and Narrow Gap Semiconductors*, edited by D. L. Carter and R. T. Bate (Pergamon, Oxford, 1971), p. 285.
- <sup>26</sup>W. Richter, T. Fjeldly, J. Renucci, and M. Cardona, *Proceedings of the International Conference on Lattice Dynamics, Paris, France*, edited by M. Balkanski (Flammarion, Paris, 1978), p. 104.
- <sup>27</sup>G. Huber, K. Syassen, and W.B. Holzapfel, *Phys. Rev. B* **15**, 5123 (1977).
- <sup>28</sup>G. J. Piermarini, S. Block, J. D. Barnett, and R. A. Forman, *J. Appl. Phys.* **46**, 2774 (1975); H. K. Mao, P. M. Bell, J. W. Shaner, and D. J. Steinberg, *ibid.* **49**, 3276 (1978).
- <sup>29</sup>*International Tables for X-ray Crystallography*, edited by T. Hahn (Reidel, Dordrecht, 1983), Vol. A.
- <sup>30</sup>F. D. Murnaghan, *Proc. Natl. Acad. Sci.* **30**, 244 (1944). The Murnaghan relation between pressure  $P$  and relative volume is  $V/V_0=(PB'/B_0+1)^{-1/B'}$ ; accordingly, for the dependence of lattice parameters  $r=a$  or  $c$  on pressure we use  $r/r_0=(PB'/\beta_0+1)^{-1/\beta}$ .
- <sup>31</sup>N. G. Pace, G. A. Saunders, and Z. Sumengen, *J. Phys. Chem. Solids* **31**, 1467 (1970).

<sup>32</sup>D. Schiferl, *Rev. Sci. Instrum.* **48**, 24 (1977).

<sup>33</sup>D. Schiferl, D. T. Cromer, and J. C. Jamieson, *Acta Crystallogr. B* **37**, 807 (1981).

<sup>34</sup>I. V. Berman and N. B. Brandt, *Pis'ma Zh. Eksp. Teor. Fiz.* **10**, 88 (1969) [*JETP Lett.* **10**, 55 (1969)].

<sup>35</sup>T. Sasaki, K. Shindo, and K. Niizeki, *Solid State Commun.* **67**, 569 (1988).

<sup>36</sup>B. Bireckoven and J. Wittig, *J. Phys. E* **21**, 841 (1988).

<sup>37</sup>Z. Wang, M. Alouani, and K. Syassen (unpublished).